Environmental Science and Pollution Research (2020) 27:5446–5455
https://doi.org/10.1007/s11356-019-06925-x

RESEARCH ARTICLE

Box-Behnken response surface approach to identify factors affecting membrane fouling in a hybrid membrane bioreactor treating domestic sewage

Ying Li[1,2,3] · Wei Chen[1,2] · Xiao-Ying Zheng[1,2] · Qiang Liu[3] · Wei Xiang[3] · Ji-Xiang Qu[4]

Received: 20 May 2019 / Accepted: 31 October 2019 / Published online: 18 December 2019

Abstract

The effect of hydraulic retention time (HRT) and sludge retention time (SRT) on extracellular polymer substrate (EPS) content and resistance of a hybrid membrane bioreactor (HMBR) treating domestic sewage was analyzed by Box-Behnken response surface methodology. The quadratic response surface model demonstrated significant effects of both HRT and SRT on EPS content (both P value < 0.05), SRT on membrane resistance (P value = 0.0119), and their interaction was significant (P value = 0.0273) for EPS but not membrane resistance (P value = 0.0609). Model optimization indicates that the optimal conditions for the HMBR to control membrane fouling were an HRT of 10 h and SRT of 30 days. Under these optimal conditions, both the EPS content and the predicted membrane resistance closely matched the actual average value with the error about 8%. Thus, the feasibility of applying response surface methodology to an HMBR for treating domestic sewage was demonstrated. According to the detection result of the three-dimensional fluorescence (excitation-emission matrix), humic acid-like and fulvic acid-like substances gain much higher levels in the suspended carriers than those in the membrane and sludge, suggesting that these are key components of the membrane pollutants.

Keywords Hydraulic retention time · Sludge retention time · Interaction effect · Excitation-emission matrix

Introduction

Hybrid membrane bioreactors (HMBRs) are specific membrane bioreactors that combine certain materials, agents, or equipment with a bioreactor (Borea et al. 2017; Mei et al. 2014; Palmarin and Young 2019). They have many advantages, including biostability, a small footprint, and a stable effluent quality despite high organic load shock (Aslam et al. 2017; Ensano et al. 2019; Park et al. 2017). However, with prolongation of the HMBR operation time, some inorganic substances, organic substances, and microorganisms including fungi, bacteria, and viruses gradually adhere to or are deposited on the inner and outer surfaces of the micromembrane, resulting in elevated filtration drag force and ultimately membrane fouling. Membrane fouling has several negative consequences, which include not only a reduction in the water production rate but also an increase in the complexity of the operation procedure. Further, the maintenance and operation cost increases, as fouling requires periodic stoppage of the membrane module from running.

HMBRs have drawn increasing research attention in the last few years to improve the design and operation conditions to avoid membrane fouling (Asif et al. 2018; Bilal et al. 2013; Jin et al. 2013; Liu et al. 2012; Loulergue et al. 2014). Despite extensive research on the membrane fouling process, including controlled experiments and simulations, it remains an inevitable outcome during HMBR operation. However, the process of membrane fouling can be slowed down by varying degrees by properly controlling the operating conditions of the reactor. Among the control parameters, sludge retention

Responsible editor: Ta Yeong Wu

✉ Xiao-Ying Zheng
zhxyqq@hhu.edu.cn

1 Key Laboratory of Integrated Regulation and Resource Development on Shallow Lake of Ministry of Education, College of Environment, Hohai University, Nanjing 210098, China

2 College of Environment, Hohai University, Nanjing 210098, China

3 School of Environmental Engineering, Xuzhou University of Technology, Xuzhou 221018, China

4 The PLA University of Science and Technology, Xuzhou 221000, China

time (SRT) has been verified to have a negligible effect on the biodegradability of the bioreactors. SRT can dominantly impact substrate concentrations, including microsecretions, biomass community, and properties of activated sludge (Gong et al. 2019; Huang et al. 2019; Huang et al. 2000; Zhang et al. 2017). Unfortunately, the association of SRT with extracellular polymeric substance (EPS) content, hydraulic resistance, and membrane fouling in HMBRs remains to be determined.

Moreover, some scholars (Cai et al. 2019; Qu et al. 2013) reported that in the process of treating domestic sewage, the treatment effects of a bioreactor are largely affected by the change in hydraulic retention time (HRT), which has a noticeable impact on mixed liquor, especially the biomass characteristics in the reaction tank, which in turn change the procedure of membrane fouling (Cai et al. 2019; Gkotsis et al. 2018; Teng et al. 2019; Yu et al. 2017). Some researchers deem that fluctuations in the HRT alter the organic loading rate (OLR); thus, the OLR varies inversely with HRT (Rahman et al. 2014; Zhang et al. 2018). However, there has been minimal research concerning the interaction between SRT and HRT, and their relative contributions to the membrane fouling mechanism. Therefore, in this study, we investigated the interaction between SRT and HRT and their influence on the biomass characteristics and membrane fouling of HMBR, including variations in the EPS content and membrane resistance.

EPS is a general term used for a variety of high molecular weight substances, and the relative molecular mass of EPSs exceeds 10,000 Da. EPSs are mainly produced by biofilm-forming bacteria through metabolism and polymerization. EPSs are generally divided into soluble EPS (S-EPS) and bound EPS (B-EPS), with the latter being subdivided into loosely bound EPS (LB-EPS) and tightly bound EPS (TB-EPS). To date, EPS and soluble microbial products (SMPs) have been considered to be the dominant substances responsible for membrane fouling (Chang and Lee 1998; Liu and Wang 2014; Ni et al. 2017). The deposition of EPS and activated sludge flocs onto the membrane surface lead to the production of a cake layer and reduction of porosity. Some scholars (Kimura et al. 2005) found that excitation/emission (Ex/Em) matrix (EEM) was effective to investigate and analyze the fouling process in membrane bioreactors. They identified a protein-like substance and humic acid-like substances at different Ex/Em by analyzing the SMP and foulants of an MBR running at various HRTs. They also indicated that SRT plays a dominant role in the characteristics of S-EPS in reactors. In the present study, both forms of EPS were detected by measuring the EPS contents in mixed liquor and biofilms of HMBRs.

Previous single-factor experiments have demonstrated that both HRT and SRT can affect EPS constitution as well as the membrane fouling process (El-Fadel et al. 2018; Liu et al. 2010). To establish optimized operating conditions and identify factors that are the main contributors of HMBR fouling, a response surface methodology (RSM) approach, which is a comprehensive experimental technique, was used. Combining systematics with statistics, an RSM approach establishes a surface model of continuous variables and also analyzes factors of the experimental design and their interactions (Antonopoulou et al. 2012; Chen et al. 2011). Thus, this approach includes experimental design, modeling, and model checking and seeks the best combination conditions along with other experimental and statistical techniques. Response surface optimization considers the random errors in experiments and fits the complex undiscovered function relations in a small range with a simple first- or second-order polynomial model. Thus, RSM serves as an efficient method to cut the expense of experiments, improve the quality of experiments, and solve practical problems in production processes, especially when the system characteristics are affected by a large number of variables. RSM approaches have been widely applied in the chemical industry, food engineering, and pharmaceutical engineering (Bhateria and Dhaka 2019; Manwar et al. 2018; Polat and Sayan 2019; Sun et al. 2019; Thakur et al. 2019). Increasing attention has been focused on industrial wastewater treatment (Rout et al. 2017; Zheng et al. 2017) instead of domestic wastewater treatment by HMBR technology. Both Box-Behnken designs (BBDs) and central composite designs (CCDs) are commonly used in RSM. BBD was selected in this study as it can be used with a lower number of experiments than CCD with the same number of factors. Therefore, we sampled five HMBRs varying in SRTs and HRTs, and determined the EPS contents in the mixed liquor and biofilm samples, along with their effects on membrane resistance. The findings of this study and the established model determined through BBD for predicting EPS may serve as a useful guide for the determination of the optimal HMBR conditions to help prevent fouling and maintain long-term membrane function.

Materials and methods

Raw wastewater

Effluent from the primary settling tank at the urban sewage treatment plant in Xuzhou, Jiangsu Province, China (longitude 117.18°, latitude 34.27°) served as the raw water in this investigation. Domestic wastewater after precipitation was used as the raw feed wastewater over a 6-month operating period, for a better analysis of the effluent organic matter characteristics under a stable condition. Table 1 lists the composition of the raw feed wastewater.

HMBR operational conditions

Five identical HMBRs worked under different SRTs and HRTs over a period of 6 months. All the HMBRs had an effective volume of 100 L; their design is schematically

Table 1 Characteristics of the raw feed wastewater

Index	Value
Temperature (°C)	14.2–25.1
pH	7.2–7.6
COD_{Cr} (mg L^{-1})	36.5–123.71
BOD_5 (mg L^{-1})	15.0–38.6
SS (mg L^{-1})	27.8–65.3
TP (mg L^{-1})	1.2–3.4
NH_4-N (mg L^{-1})	10.6–27.8
TN (mg L^{-1})	13.9–34.2

Table 2 HMBR operating conditions

Working volume	1 m^3
Biological padding volume fraction	50.0%
Hydraulic retention time (HRT)	6 h, 8 h, 10 h
Solid retention time (SRT)	10, 20, 30 days
Initial SRT	10
Membrane area	10.0 m^2
Membrane effective pore size	0.1 μm
Membrane flux	10.0, 12.5, 16.7 L m^{-2} h^{-1}
pH	7.5
Dissolved oxygen	4.0 mg L^{-1}
Temperature	20.0 °C

presented in Fig. 1, and the operating conditions are shown in Table 2. A polyvinylidene (PVDF) hollow fiber membrane with an average pore size of 0.10 mm was immersed in the mixture. Polyethylene K_3 biological fillers, with a porous interior cylinder (diameter 25 mm and height 12 mm), were placed in the tank, with a 50% (volume fraction) dose. Air was transferred into the liquid phase through the diffusers at the bottom of the vessel with a velocity of 2 m^3 per membrane area (m^2) per hour. This method of aeration not only provides oxygen for microbial metabolism but also able to scour the membranes and alleviate the attachment of deposits. The concentration of dissolved oxygen (DO) in the mixture was controlled at approximately 4 mg L^{-1} by aeration from the diffuser on the bottom through an air flow meter. The temperature of the mixture was controlled at approximately 20 °C using a heating rod. The membrane module was operated by a self-priming pump, under constant water flux of 10.0, 12.5, and 16.7 L m^{-2} h^{-1}, respectively, according to the different HRTs with a 10-min operation cycle (8 min on, 2 min off). When TMP achieved 20 kPa, the membrane module was considered to be contaminated and then was brought out for chemical cleaning by using Deng's method (Deng et al. 2016).

Analysis methods

Water quality measurement

To determine the quality of the raw feed wastewater, the temperature and pH values were determined by a pH analyzer (pH Meter, ARCO Electronics LTD, Guangdong). COD_{Cr}, BOD_5, SS, NH_4^+-N, TP, and TN were analyzed according to standard methods (APHA, 2005). Our previous studies showed that HMBR performed well in treating domestic wastewater (Li et al. 2019), and thus, the optimum operating condition based on effluent quality analysis were not a concern in this study. Instead, HRT and SRT were applied to analyze the mechanism of membrane fouling influence.

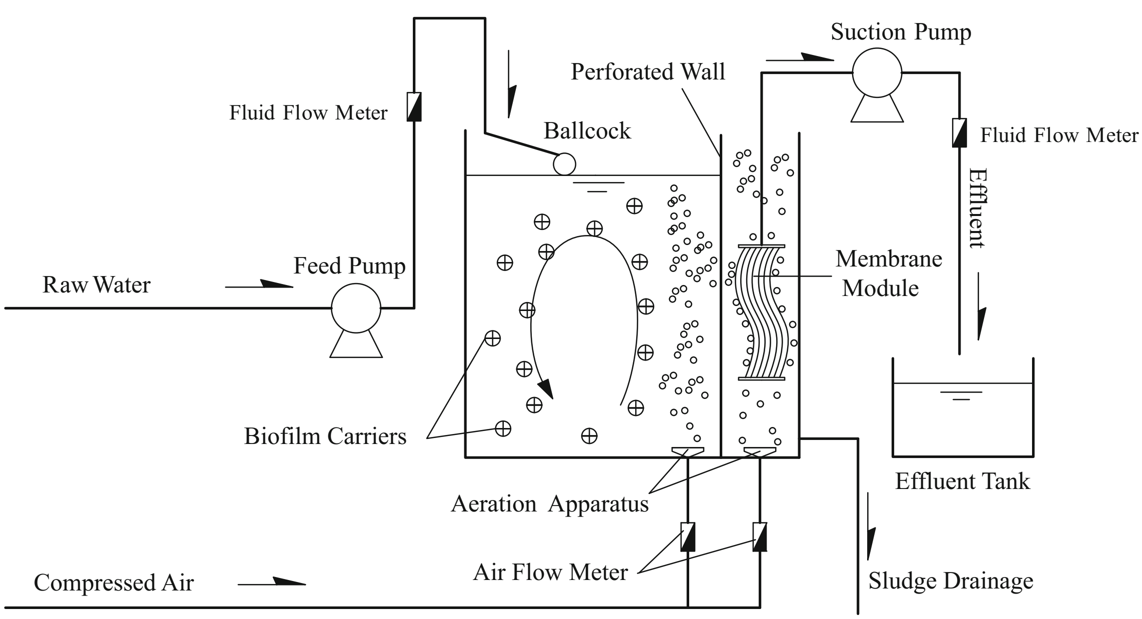

Fig. 1 Schematic of the HMBR system

Table 3 Factors and levels of response surface analysis

Factor	Coded		
	− 1	0	1
A/h	6	8	10
B/d	10	20	30

EPS extraction and detection

Five milliliters of the mixed liquor was filtered through a 0.22-mm pore-size filter paper, and the DOC of the filtrate was considered to be S-EPS. LB-EPS quantity, calculated by subtracting the S-EPS amount from the EPS amount of the filtrate, was obtained by determining the supernatant DOC value after high-speed centrifugation. The specific operating conditions were described previously (Li et al. 2019). To supplement the loss of water after the previous filtration, 5 mL of pure water was injected into the centrifuge tube. A water bath under 80 °C was used to heat the well-mixed solution for 30 min. The sample was then centrifuged at 8311.68*g* for 20 min, and the supernatant was filtered through a 0.22-μm pore-size filter paper. This filtrate was used to measure the EPS components of mixed liquor.

The biofilm slicked to the suspended filter was scraped and enriched smoothly by a plastic sheet. A mixture of a certain concentration composed of the enriched biofilm and deionized water was placed into a test tube to detect the quantity of the EPS. Because S-EPS was absent in the biofilm, only LB-EPS and TB-EPS were measured, which were extracted from the biofilms in the same manner as described above for the mixed liquid. The amount of EPS was typically quantified by milligrams per unit mass volatile suspended solid (VSS).

The EEMs of the obtained EPS from the mixed liquid and biofilm were assessed using a fluorescence spectrophotometer (Shanghai Sanke Electrical Appliances Co., Ltd.). The excitation wavelength ranged from 200 to 500 nm, and the emission wavelength ranged from 280 to 500 nm; 5-nm increments for both Ex and Em models were applied to obtain the spectra.

Test of membrane resistance

After each operation cycle, the contaminated membrane module was brought out from the tank and washed by pure water to remove the biofilm and sludge attached to the membranes. The membrane resistance was calculated by laying the membrane module in deionized water and operating it at various fluxes. Total resistance (R_t) during membrane filtration mainly comprises inherent resistance (R_m), pore resistance (R_p), and cake layer resistance (R_c), which were respectively calculated by using Lee's method (Lee et al. 2003).

RSM and statistical analysis

The RSM was developed by Box and collaborators in the 1950s (Polat and Sayan 2019). Mathematical and statistical techniques are used in RSM to match empirical models to experimental data. To achieve this goal, linear or square functions were used to represent the system studied and, consequently, to search the optimum solution. Box and Behnken (1960) proposed methods to opt points from three-level factorial arrays, which are called BBD and can make models more efficient and profitable compared to their corresponding 3^k designs, mainly due to consideration of a large number of factors. More information on the theoretical principles of

Table 4 RSM experimental design and results of membrane fouling

Run	Factor 1 *A*:HRT (h)	Factor 2 *B*:SRT (days)	Response 1 EPS (mg g^{-1}VSS)	Response 2 membrane resistance (10^{12} m^{-1})
1	6.00	20.00	101.5	5.84
2	10	10.00	128.3	7.83
3	8.00	10.00	135.1	8.91
4	8.00	20.00	78.0	4.14
5	8.00	30.00	79.6	3.31
6	10.00	20.00	42.3	4.05
7	6.00	30.00	95.3	4.41
8	8.00	20.00	85.0	5.14
9	8.00	30.00	62.5	5.98
10	10.00	30.00	43.6	3.24
11	6.00	20.00	100.2	4.98
12	8.00	20.00	86.3	4.62
13	6.00	10.00	105.7	3.57
14	8.00	10.00	99.4	7.69
15	10.00	20.00	72.3	4.95

Table 5 ANOVA for response surface linear model: response 1 EPS content

Source	Sum of squares	*df*	Mean square	*F* value	*P* value Prob > *F*	
Model	7462.46	3	2487.49	11.67	0.0010	Significant
A	1687.81	1	1687.81	7.92	0.0169	
B	4394.53	1	4394.53	20.61	0.0004	
AB	1380.12	1	1380.12	6.47	0.0273	
Residual	2445.39	11	213.22			
Lack of fit	1071.87	5	214.37	1.01	0.4850	Not significant
Pure error	1273.52	6	212.25			
Cor total	9807.85	14				
	R^2 = 0.7609, R^2_{Adj} = 0.6956, *C.V.* = 16.66%					

RSM and procedures for its function can be found in the report by Dun et al.'s (2014). According to the BBD principle, the response surface experiments of three factors and three levels were designed using Design Expert software (Version 12) with EPS content and the membrane resistance coefficient as the response values Y_1 and Y_2, respectively. HRT (*A*) and SRT (*B*) were selected as the two influencing factors. Table 3 shows the factors and levels used in the response surface analysis.

The experimental data of EPS content shown in Table 3 were fitted to the model and tested using analysis of variance (ANOVA), and the quadratic regression models of *A* and *B* for EPS content were obtained.

Results and analysis

Response surface design

EPS, as an important component of membrane pollutants in an HMBR, together with the membrane resistance coefficient, is an important comprehensive index to characterize the degree of membrane fouling. HRT and SRT are important indicators of membrane fouling.

According to the experimental factors and levels established using Design Expert software, the experimental values of surface modification conditions optimized by RSM are shown in Table 4, including a total of 15 experimental points.

Regression model and ANOVA

The final equations of the regression models with the coded factors (Table 3) were as follows:

$$\text{EPS content} = 87.67-14.53A-23.44B-18.577AB$$

$$\text{Membrane Resistanceresistance} = 5.24 + 0.1587A-1.38B-1.36AB$$

The ANOVA results for model fitting are shown in Tables 5, 6, 7, and 8. For EPS, the *F* value of the model was 11.67, demonstrating that the model is statistically significant (P = 0.0010). The lack of fit *F* value of 1.01 signified that the lack of fit is not significant relative to the pure error probability. Specifically, there was a 48.50% chance that a lack of fit *F* value this large could occur due to noise. Nonsignificant lack of fit is good.

Similarly, for membrane resistance, *B* was found to be significant (P = 0.0119), with a lack of fit *F* value of 2.80 indicating no significant lack of fit relative to the pure error, and a 12.14% chance that this lack of fit could be due to noise.

Table 6 ANOVA for response surface linear model: response 2 membrane resistance

Source	Sum of Squares	*df*	Mean Square	*F* Value	*P*-value Prob > *F*	
Model	22.86	3	7.62	4.51	0.0270	Significant
A	0.2016	1	0.2016	0.1192	0.7364	
B	15.29	1	15.29	9.04	0.0119	
AB	7.37	1	7.37	4.36	0.0609	
Residual	18.60	11	1.69			
Lack of fit	13.01	5	2.60	2.80	0.1214	Not significant
Pure error	5.58	6	0.9306			
Cor total	41.46	14				
	R^2 = 0.5514, R^2_{Adj} = 0.4291, *C.V.* = 24.80%					

Table 7 Test of significance for coefficients of the quadratic model: response 1 EPS content

Factor	Coefficient estimate	*df*	Standard error	95% CI low	95% CI high	VIF
Intercept	87.67	1	3.77	79.37	95.96	
A	− 14.53	1	5.16	− 25.89	− 3.16	1.00
B	− 23.44	1	5.16	− 34.80	− 12.07	1.00
AB	− 18.57	1	7.30	− 34.64	− 2.51	1.00

ANOVA of the regression model showed that the linear terms *A* and *B* of the model could significantly influence response factor 1, and linear term *B* could significantly influence response factor 1 but not factor 2. In the quadratic term, the effect of *AB* could significantly correlate with response factors 1 and 2.

3D response surface graph and contour graph analysis

Effect of HRT and SRT on EPS

The effect of HRT and SRT on the EPS contents is presented in Figs. 2, 3, 4, and 5 in the form of response surface graphs. These results demonstrated that when the HRT is less than 10 h and is kept constant, the change in EPS contents decreases slowly with the extension of SRT. However, when the HRT is greater than 10 h, the EPS content exhibits an initial decrease, followed by an increase with the extension of SRT. Higher fouling rates in terms of EPS content can be ascribed to higher pollutant loading rates (increased F/M) and inadequate retention time with shorter HRT (Deng et al. 2016). As the supply of organic matter exceeds the demand of consumption, immobilized microorganisms grow at the maximum speed on the carrier surface, and the yield of biofilm polysaccharide and protein increases (Cai et al. 2019; Gkotsis et al. 2018; Huang et al. 2019). The B-EPS is closely related to growth and is generated in a direct proportion to substrate utilization (Qu et al. 2013). Therefore, the decreased HRT facilitates the generation of bound EPS and eventually increases the total content of EPS (Hao et al. 2016).

Excessive and low F/M affects the microbial count, which in turn may affect the production of EPS. The change in SRT may lead to a change in MLSS, MLVSS, and MLVSS/MLSS. A high MLVSS/MLSS ratio after a long SRT (30 days) indicates high viability of biomass from the perspective of assimilation and decomposition (Li et al. 2006; Liu et al. 2012).When SRT is too short or F/M is too high, organic matter, and nutrients are converted into EPS before they can be completely consumed by microorganisms (Burman and Sinha 2018; Choi et al. 2013; Li et al. 2019); on the contrary, endogenous respiration of microorganisms can intensify and produce a substantial amount of EPS. In this study EPS increased with decreasing SRT, indicating that there may be more utilization-associated SMPs at short SRTs (high F/M ratio). The microbial activities of biomass were positively correlated with bound EPS and SMP, which is consistent with the study of Choi's studies (Choi et al. 2013).

Effect of HRT and SRT on membrane resistance

The total hydraulic resistance for each membrane module was calculated based on Eq. (1).

$$R_T = R_M + R_C + R_P \quad (1)$$

where R_T (m^{-1}) is the total membrane resistance, R_M (m^{-1}) is the intrinsic membrane resistance, R_C (m^{-1}) is the cake resistance, and R_P (m^{-1}) is the pore blocking resistance.

As shown in Figs. 2, 3, 4, and 5, R_T showed the same pattern of change as that of EPS content to a great extent. This indicated that EPS is closely related to membrane resistance, which is consistent with previous reports (Dong et al. 2018; Teng et al. 2019). The main reason for the increase in membrane resistance is that EPS is adsorbed on the surface of the membrane or inside the channel (Nouha et al. 2018; Tansel et al. 2006). With the increase in adsorption capacity, the pore size of the membrane becomes increasingly and more severely blocked, resulting in a continuous increase in membrane resistance (Chabaliná et al. 2013). Among the components of EPS, S-EPS, and LB-EPS play an important role in membrane fouling. Reduction of S-EPS may lead to the reduction of R_P and R_C (Borea et al. 2017). Reduction of LB-EPS can ameliorate the flocculation and sedimentation performance of activated sludge (Su et al. 2014). Flocculation performance is

Table 8 Test of significance for coefficients of the quadratic model: response 2 membrane resistance

Factor	Coefficient estimate	*df*	Standard error	95% CI low	95% CI high	VIF
Intercept	5.24	1	0.3357	4.51	5.98	
A	0.1587	1	0.4597	− 0.8531	1.17	1.0000
B	− 1.38	1	0.4597	− 2.39	− 0.3707	1.0000
AB	− 1.36	1	0.6501	− 2.79	0.0735	1.0000

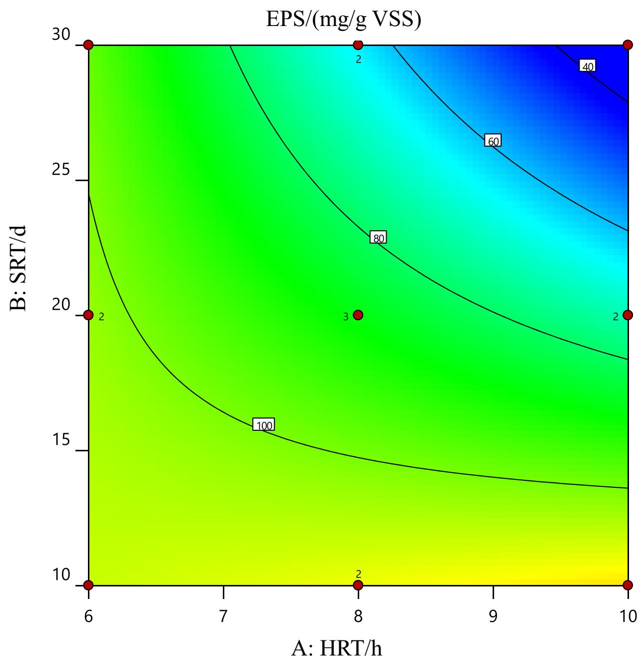

Fig. 2 Contour graph of HRT and SRT on EPS content

improved when the number of colloids in water decreases and R_P decreases further. Therefore, R_C, R_P, and R_T gradually decrease with the reduction of S-EPS and LB-EPS.

Lower operating flux (longer HRT) generated small drag force for the particles, which could help form a loose gel layer rather than a compact cake layer (Gkotsis et al. 2018). Appropriate extension of SRT was considered to be conducive to the accumulation of total biomass, but continuous prolongation of SRT (lower F/M) aggravates endogenous microbial respiration and causes elevation of EPS levels. The increased EPS would strengthen the polymer bridging of sludge flocs and embed small flocs in the EPS matrix, thus hindering deflocculation and small floc production (Huang et al. 2019; Liu et al. 2012). Thus, our results suggested that appropriate extension of HRT and SRT is conducive to controlling membrane fouling; however, when the HRT exceeds 8 h, an SRT of over 30 days may have the opposite effect.

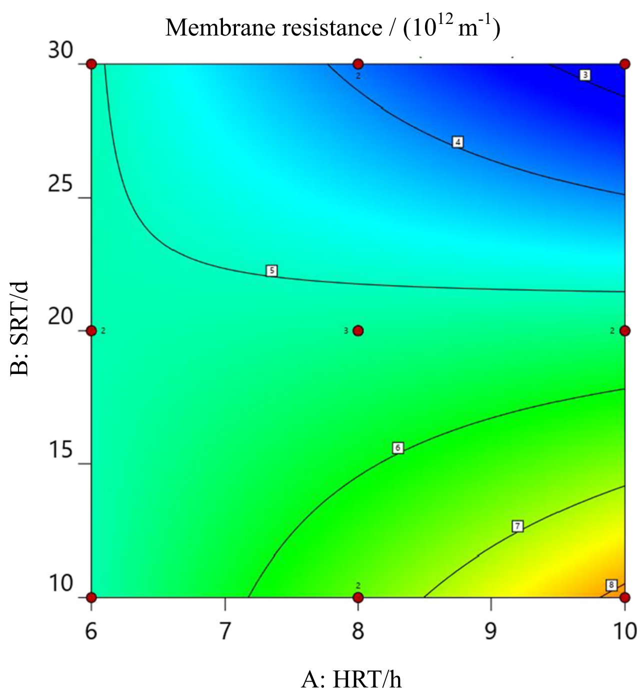

Fig. 3 Contour graph of HRT and SRT on membrane resistance

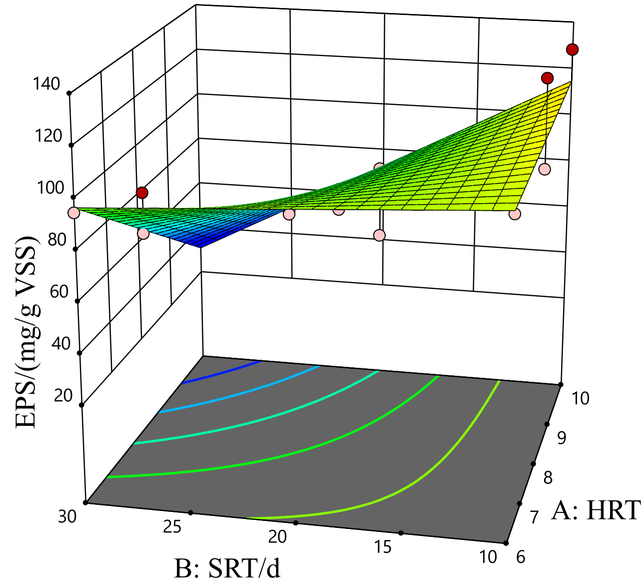

Fig. 4 3D response surface graph of HRT and SRT on EPS content

Determination and verification of optimum operating conditions

Based on the above results, the optimum conditions of HMBR were determined to be an HRT of 9.53 h and SRT of 29.77 days, corresponding to an EPS content and membrane

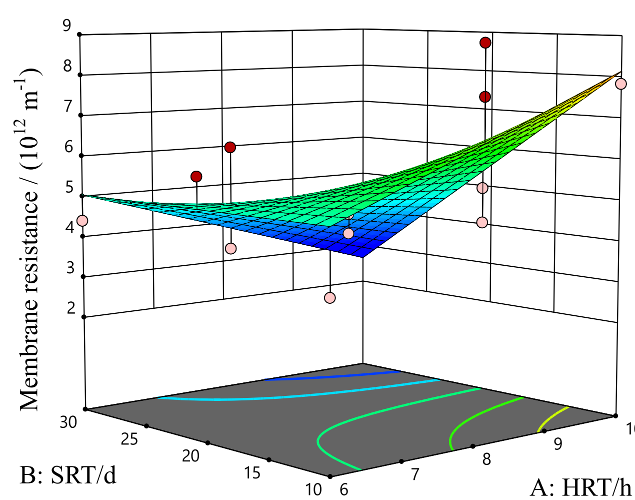

Fig. 5 3D response surface graph of HRT and SRT on membrane resistance

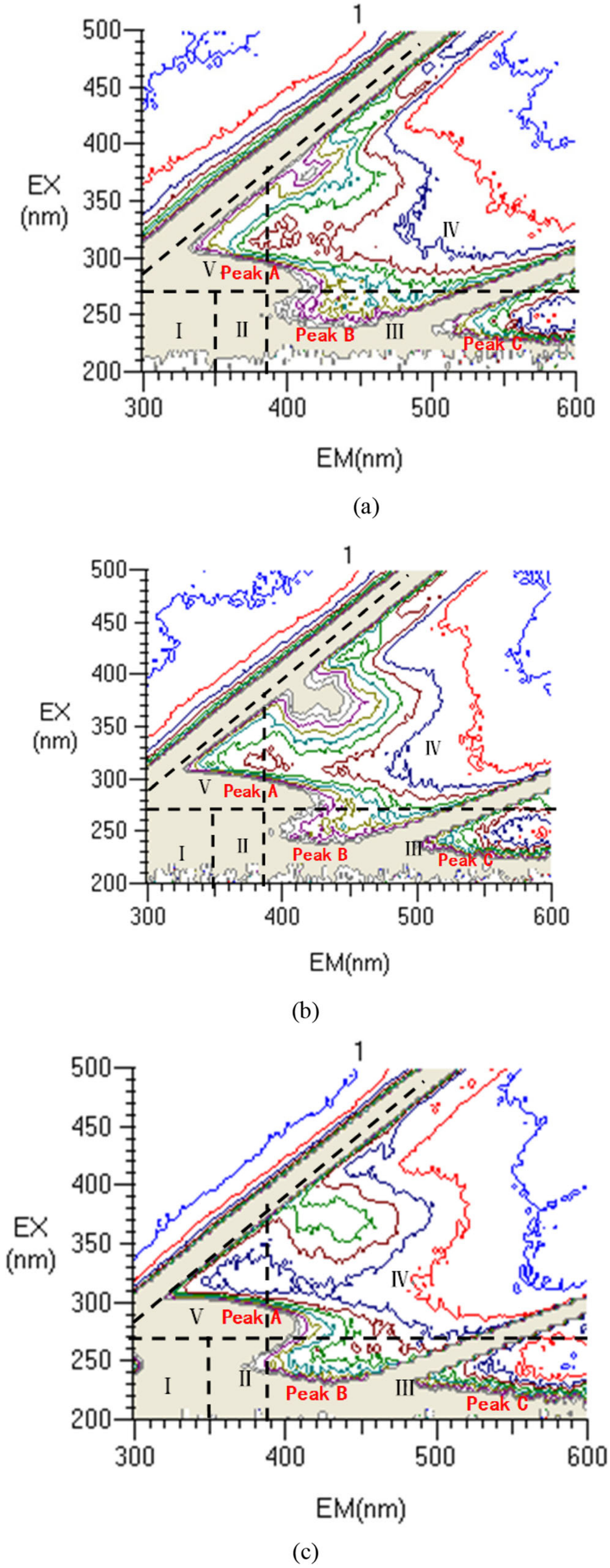

Fig. 6 Excitation emission matrix (EEM) spectra of membrane foulant of suspended carrier (**a**), membrane (**b**), and sludge (**c**) in wastewater treatment

resistance of 39.80 mg g^{-1} VSS and 3.21 × 10^{12} m^{-1}, respectively. Considering the feasibility and convenience of practical operation, the simulated operating conditions were revised as follows: HRT of 8 h and SRT of 30 days. To test and verify the reliability of the simulation based on RSM, membrane fouling control experiments were carried out under the optimum operating conditions. The EPS content of the three repeated experiments was found to be 43.17 mg g^{-1} VSS and the membrane resistance was 3.46 × 10^{12} m^{-1}, which are consistent with the predicted values of the model. Therefore, the optimal operating conditions obtained by the RSM were confirmed to be accurate and reliable, with potential practical value.

Characteristics of membrane fouling components under the optimal operating conditions

The EEM analysis was further applied to investigate EPS in the components and structures of the suspended carrier, membrane, and sewage sludge under the optimum operating conditions (Fig. 6). Three major peaks could be read from the fluorescence spectra. The first major peak was located at the Ex/Em wavelengths of 340–360/420–445 nm (peak A), which is considered a visible humic acid-like fluorescence. The second major peak was located at the Ex/Em wavelengths of 250–260/430–460 nm (peak B), which is regarded as a fulvic acid-like or unknown fluorescent component of humus. Moreover, a third major peak was observed at Ex/Em of 240–260/570–600 nm (Peak C), which was used to characterize the unknown fluorescent components. The peaks located at Ex/Em of 225/340 nm and 230/430 nm can be used for online analysis and real-time monitoring of NH_4^+-N and TN in municipal domestic sewage. Since no such peaks were detected in the three samples in this research, the nitrogen removal effect of the HMBRs could be considered to be good. The characteristic humic acid peak (peak A) showed a relatively high content in suspended carriers, followed by the membrane and sludge. The main components of humic acid are high polymers of aliphatic and aromatic groups. Functional groups, such as carboxyl and phenol groups, which originate from ion dissociation and exchange with hydrogen ions in solution, result in high negative charges. This consequently weakens the flocculation ability of the sludge, and is not conducive to sludge granulation. Optimum SRT should be confirmed between 20 days and 30 days to improve settling performance.

Conclusion

Based on a previous single-factor experiment, a quadratic multiple regression model of the influence of HRT and SRT changes on the EPS content and membrane resistance of HMBRs was established using an RSM method. The influences of the two factors were pronounced, as was their interaction. The model was confirmed to be reasonable and reliable. According to the model optimization and practical feasibility, the optimal HRT is 10 h and SRT is 30 days. Under the optimal working condition, the EPS content was 43.17 mg g^{-1} VSS and the membrane resistance was 3.46 × 10^{12} m^{-1}, which indicated that the empirical model established by the RSM has a better regression fit. The EEM results further indicated that humic acid-like and fulvic acid-like were the dominant composition of EPS in the HMBR, which likely conducive to format and keep structural stability of the biofilm. Later studies for membrane fouling control can be carried out from the perspective of controlling the secretion of humic acids and humic acids by microorganisms.

Acknowledgments Firstly, we appreciate all the reviewers and editors valuable comments and suggestions on revising and improving the work.

Funding information This study is financially supported by the following: Jiangsu Ministry of Housing and Urban and Rural Construction Project (No. 00730091), the Jiangsu Natural Science Foundation (No. BK20151161), major projects of Natural Science Research in Jiangsu higher education institutions (No. 17KJA610004), Qinglan Project in Jiangsu Province, A Project Funded by the Priority Academic Program Development of Jiangsu Higher Education Institutions (PAPD), Scientific Research Projects of Xuzhou Institute of Engineering (No. XKY2013106, XKY2018245), and Xuzhou Science and Technology Project (No. KC16SQ192, No. KC19047).

References

Antonopoulou M, Papadopoulos V, Konstantinou I (2012) Photocatalytic oxidation of treated municipal wastewaters for the removal of phenolic compounds: optimization and modeling using response surface methodology (RSM) and artificial neural networks (ANNs). J Chem Technol Biotechnol 87:1385–1395. https://doi.org/10.1002/jctb.3755

Asif MB, Ansari AJ, Chen SS, Nghiem LD, Price WE, Hai FI (2018) Understanding the mechanisms of trace organic contaminant removal by high retention membrane bioreactors: a critical review. Environ Sci Pollut Res:1–16. https://doi.org/10.1007/s11356-018-3256-8

Aslam M, Charfi A, Lesage G, Heran M, Kim J (2017) Membrane bioreactors for wastewater treatment: A review of mechanical cleaning by scouring agents to control membrane fouling. Chem Eng J 307:897–913. https://doi.org/10.1016/j.cej.2016.08.144

Bhateria R, Dhaka R (2019) Optimization and statistical modelling of cadmium biosorption process in aqueous medium by Aspergillus niger using response surface methodology and principal component analysis. Ecol Eng 135:127–138. https://doi.org/10.1016/j.ecoleng.2019.05.010

Bilal M et al (2013) Waste biomass adsorbents for copper removal from industrial wastewater—a review. J Hazard Mater 263:322–333

Borea L, Naddeo V, Belgiorno V (2017) Application of electrochemical processes to membrane bioreactors for improving nutrient removal and fouling control. Environ Sci Pollut Res 24:321–333. https://doi.org/10.1007/s11356-016-7786-7

Burman I, Sinha A (2018) A review on membrane fouling in membrane bioreactors: control and mitigation. Environ Contam:281–315. https://doi.org/10.1007/978-981-10-7332-8_13

Cai Y, Li X, Zaidi AA, Shi Y, Zhang K, Feng R, Lin A, Liu C (2019) Effect of hydraulic retention time on pollutants removal from real ship sewage treatment via a pilot-scale air-lift multilevel circulation membrane bioreactor. Chemosphere 236:124338. https://doi.org/10.1016/j.chemosphere.2019.07.069

Chabaliná LD, Pastor MR, Rico DPJT (2013) Characterization of soluble and bound EPS obtained from 2 submerged membrane bioreactors by 3D-EEM and HPSEC. Talanta 115:706–712

Chang I-S, Lee C-HJD (1998) Membrane filtration characteristics in membrane-coupled activated sludge system—the effect of physiological states of activated sludge on membrane fouling. Desalination 120:221–233

Chen Y, Lin CJ, Jones G, Fu S, Zhan H (2011) Application of statistical design for the optimization of microbial community of synthetic domestic wastewater. Biodegradation 22:205–213. https://doi.org/10.1007/s10532-010-9388-2

Choi BG, Cho J, Song KG, Maeng SK (2013) Correlation between effluent organic matter characteristics and membrane fouling in a membrane bioreactor using advanced organic matter characterization tools. Desalination 309:74–83. https://doi.org/10.1016/j.desal.2012.09.018

Deng L et al (2016) Effects of hydraulic retention time and bioflocculant addition on membrane fouling in a sponge-submerged membrane bioreactor. Bioresour Technol 210:11–17. https://doi.org/10.1016/j.biortech.2016.01.056

Dong Z, Shang W, Dong W, Zhao L, Li M, Wang R, Sun F (2018) Suppression of membrane fouling in the ceramic membrane bioreactor (CMBR) by minute electric field. Bioresour Technol 270:113–119. https://doi.org/10.1016/j.biortech.2018.08.087

El-Fadel M, Sleem F, Hashisho J, Saikaly PE, Alameddine I, Ghanimeh S (2018) Impact of SRT on the performance of MBRs for the treatment of high strength landfill leachate. Waste Manag 73:165–180. https://doi.org/10.1016/j.wasman.2017.12.003

Ensano BMB, Borea L, Naddeo V, de Luna MDG, Belgiorno V (2019) Control of emerging contaminants by the combination of electrochemical processes and membrane bioreactors. Environ Sci Pollut Res 26:1103–1112. https://doi.org/10.1007/s11356-017-9097-z

Gkotsis P, Tsilogeorgis J, Zouboulis A (2018) Hydraulic performance and fouling characteristics of a membrane sequencing batch reactor (MSBR) for landfill leachate treatment under various operating conditions. Environ Sci Pollut Res 25:12274–12283. https://doi.org/10.1007/s11356-017-0142-8

Gong H, Jin Z, Xu H, Yuan Q, Zuo J, Wu J, Wang K (2019) Enhanced membrane-based pre-concentration improves wastewater organic matter recovery: pilot-scale performance and membrane fouling. J Clean Prod 206:307–314. https://doi.org/10.1016/j.jclepro.2018.09.209

Hao L, Liss SN, Liao BQ (2016) Influence of COD:N ratio on sludge properties and their role in membrane fouling of a submerged membrane bioreactor. Water Res 89:132–141. https://doi.org/10.1016/j.watres.2015.11.052

Huang X, Liu R, Qian YJPB (2000) Behaviour of soluble microbial products in a membrane bioreactor. Process Biochem 36:401–406

Huang J et al (2019) Linking solids retention time to the composition, structure, and hydraulic resistance of biofilms developed on support materials in dynamic membrane bioreactors. J Membr Sci 581:158–167. https://doi.org/10.1016/j.memsci.2019.03.033

Jin L, Ong SL, Ng HY (2013) Fouling control mechanism by suspended biofilm carriers addition in submerged ceramic membrane bioreactors. J Membr Sci 427:250–258. https://doi.org/10.1016/j.memsci.2012.09.016

Kimura K, Yamato N, Yamamura H, Watanabe YJEs, technology (2005) Membrane fouling in pilot-scale membrane bioreactors (MBRs) treating municipal wastewater. Environ Sci Technol 39:6293–6299

Lee W, Kang S, Joms SHJ (2003) Sludge characteristics and their contribution to microfiltration in submerged membrane bioreactors. J Membr Sci 216:217–227

Li H, Yang M, Zhang Y, Yu T, Kamagata Y (2006) Nitrification performance and microbial community dynamics in a submerged

membrane bioreactor with complete sludge retention. J Biotechnol 123:60–70. https://doi.org/10.1016/j.jbiotec.2005.10.001
Li Y, Chen W, Liu Q, Xiang W, Zheng X-C, Qu J-X (2019) Effect on composition and quantity of extracellular polymeric substances in an innovative hybrid membrane bioreactor under different sludge retention times. Environmental Pollutants and Bioavailability 31: 103–111. https://doi.org/10.1080/26395940.2019.1587314
Liu Q, Wang XC (2014) Mechanism of nitrogen removal by a hybrid membrane bioreactor in municipal wastewater treatment. Desalin Water Treat 52:5165–5171. https://doi.org/10.1080/19443994.2014.927186
Liu Q, Wang XC, Liu Y, Yuan H, Du Y (2010) Performance of a hybrid membrane bioreactor in municipal wastewater treatment. Desalination 258:143–147. https://doi.org/10.1016/j.desal.2010.03.024
Liu Y, Liu H, Cui L, Zhang KJD (2012) The ratio of food-to-microorganism (F/M) on membrane fouling of anaerobic membrane bioreactors treating low-strength wastewater. Desalination 297:97–103
Loulergue P, Weckert M, Reboul B, Cabassud C, Uhl W, Guigui CJW (2014) Mechanisms of action of particles used for fouling mitigation in membrane bioreactors. Water Res 66:40–52
Manwar JV, Vispute SS, Kumbhar DD, Manmode RS, Bakal RL, Jadhao RG, Jogdand SD (2018) Response surface based optimization of system variables for liquid chromatographic analysis of candesartan cilexetil. Journal of Taibah University for Science 11:159–172. https://doi.org/10.1016/j.jtusci.2016.02.004
Mei X, Wang Z, Zheng X, Huang F, Ma J, Tang J, Wu ZJ (2014) Soluble microbial products in membrane bioreactors in the presence of ZnO nanoparticles. J Membr Sci 451:169–176
Ni L, Li D, Rong S, Su L, Zhou W, Wang P, Wang C, Li S, Acharya K (2017) Characterization of extracellular polymeric substance (EPS) fractions produced by Microcystis aeruginosa under the stress of linoleic acid sustained-release microspheres. Environ Sci Pollut Res 24:21091–21102. https://doi.org/10.1007/s11356-017-9540-1
Nouha K, Kumar RS, Balasubramanian S, Tyagi RD (2018) Critical review of EPS production, synthesis and composition for sludge flocculation. J Environ Sci (China) 66:225–245. https://doi.org/10.1016/j.jes.2017.05.020
Palmarin MJ, Young S (2019) Comparison of the treatment performance of a hybrid and conventional membrane bioreactor for greywater reclamation. Journal of Water Process Engineering 28:54–59. https://doi.org/10.1016/j.jwpe.2018.12.012
Park D, Yun Y-M, Kim H, Choi S, Kang SJD, TREATMENT W (2017) Mechanism of biofouling mitigation on nanofiltration membrane by non-oxidizing biocide. Desalin Water Treat 99:102–106
Polat S, Sayan P (2019) Application of response surface methodology with a Box–Behnken design for struvite precipitation. Adv Powder Technol 30:2396–2407. https://doi.org/10.1016/j.apt.2019.07.022
Qu X, Gao WJ, Han MN, Chen A, Liao BQ (2013) Effect of hydraulic retention time on sludge properties, cake layer structure, and membrane fouling in a thermophilic submerged aerobic membrane bioreactor. Sep Sci Technol 48:1529–1536. https://doi.org/10.1080/01496395.2012.749284
Rahman RA, Molla AH, Fakhru'l-Razi A (2014) Assessment of sewage sludge bioremediation at different hydraulic retention times using mixed fungal inoculation by liquid-state bioconversion. Environ Sci Pollut Res 21:1178–1187. https://doi.org/10.1007/s11356-013-1974-5
Rout PR, Puspendu B, Dash RR (2017) Response surface optimization of phosphate removal from aqueous solution using a natural adsorbent. Trends in Asian water Environmental Science and Technology Environ. Sci. Technol:93–104
Su X, Tian Y, Zuo W, Zhang J, Li H, Pan XJW (2014) Static adsorptive fouling of extracellular polymeric substances with different membrane materials. Water Res 50:267–277
Sun Y, Yang Y, Yang M, Yu F, Ma J (2019) Response surface methodological evaluation and optimization for adsorption removal of ciprofloxacin onto graphene hydrogel. J Mol Liq 284:124–130. https://doi.org/10.1016/j.molliq.2019.03.118
Tansel B, Sager J, Garland J, Xu S, Levine L, Bisbee P (2006) Deposition of extracellular polymeric substances (EPS) and microtopographical changes on membrane surfaces during intermittent filtration conditions. J Membr Sci 285:225–231. https://doi.org/10.1016/j.memsci.2006.08.031
Teng J, Zhang M, Leung KT, Chen J, Hong H, Lin H, Liao BQ (2019) A unified thermodynamic mechanism underlying fouling behaviors of soluble microbial products (SMPs) in a membrane bioreactor. Water Res 149:477–487. https://doi.org/10.1016/j.watres.2018.11.043
Thakur RK, Sharma D, Singh KK (2019) Optimization of surface roughness and delamination factor in end milling of graphene modified GFRP using response surface methodology. Materials Today: Proceedings. https://doi.org/10.1016/j.matpr.2019.06.153
Yu D, Chen Y, Wei Y, Wang J, Wang Y, Li K (2017) Fouling analysis of membrane bioreactor treating antibiotic production wastewater at different hydraulic retention times. Environ Sci Pollut Res 24: 9026–9035. https://doi.org/10.1007/s11356-015-5751-5
Zhang DQ, Eng CY, Stuckey DC, Zhou Y (2017) Effects of ZnO nanoparticle exposure on wastewater treatment and soluble microbial products (SMPs) in an anoxic-aerobic membrane bioreactor. Chemosphere 171:446–459. https://doi.org/10.1016/j.chemosphere.2016.12.053
Zhang D, Trzcinski AP, Luo J, Stuckey DC, Tan SK (2018) Fate and behavior of dissolved organic matter in a submerged anoxic-aerobic membrane bioreactor (MBR). Environ Sci Pollut Res 25: 4289–4302. https://doi.org/10.1007/s11356-017-0586-x
Zheng Y, Xing M, Cai L, Xiao T, Lu Y, Jiang J (2017) Interaction of earthworms-microbe facilitating biofilm dewaterability performance during wasted activated sludge reduction and stabilization. Sci Total Environ 581-582:573–581. https://doi.org/10.1016/j.scitotenv.2016.12.166

Publisher's note Springer Nature remains neutral with regard to jurisdictional claims in published maps and institutional affiliations.